Mechanics of Advanced Composite Structures 5 (2018) 141 – 147

Mechanics of Advanced Composite Structures

journal homepage: http://MACS.journals.semnan.ac.ir

Semnan University

Creep Strain and Stress Analysis in Laminated Composite Pressure Vessels

A.R. Ghasemi*, K. Hosseinpour

Composite and Nanocomposite Research Laboratory, Department of Solid Mechanics, Faculty of Mechanical Engineering, University of Kashan, Kashan, 87317-53153, Iran

PAPER INFO

Paper history:
Received 2017-09-21
Received in revised form 2018-01-07
Accepted 2018-01-29

Keywords:
Long-term creep strain
Schapery single integral
Nonlinear viscoelastic
Polymer matrix composites

ABSTRACT

This study investigates the time-dependent long-term creep strain in a composite cylinder made of glass/vinylester with a unidirectional ply. The cylinder is subjected to an internal pressure and the boundary condition is free–free and acts as thermal insulation. The classical lamination theory (CLT) is used to derive the governing equations as a second-order equation to determine the radial, circum-ferential, axial, and effective stresses in the cylinder wall. The distribution of the radial and circumferential creep strains is based on the Schapery's single integral model for nonlinear viscoelastic materials. This study focuses on the effect of the orientation of the fibers on the creep strain distribution in the wall of a cylinder. The results show that the creep strain is lower when $\theta = 45°$ than at $\theta = 90°$. As the angle of the fibers increases, the distribution of the creep strain becomes more uniform.

1. Introduction

Many studies have been done on the cylindrical structure because it is one of the most widely used structures in industry [1, 2]. Laminated composite materials (LCMs) have superior specific properties regarding their stiffness and strength, and tend to replace the traditional materials used for the construction of structural components in several engineering fields. Tsukrov and Drach [3] investigated the elastic deformation of laminated composite cylinders that were subjected to homogeneous boundary conditions. Zhang et al. [4] investigated the thermomechanical stresses in a multilayered composite pressure vessel. They derived an analytical solution for determining the stress–strain distribution of a laminated composite pressure vessel subjected to internal pressure and a thermal load. Ghasemi et al. [5] performed analytical and numerical investigations of functionally graded materials (FGMs) reinforced by LCMs using the infinitesimal theory of elasticity. Arefi et al. [6, 7] studied the two-dimensional thermoelastic analysis of a functionally graded cylindrical shell subjected to uniform and nonuniform mechanical and thermal loads.

Designing for the long-term durability of composite structures requires an understanding of the viscoelastic behavior of the composite materials and how it affects strength. Compared with the elastic properties of the LCMs, the time-dependent and creep properties are extremely weak. Violette and Schapery [8] studied the time-dependent compressive strength of unidirectional viscoelastic composite materials and the long-term durability of unidirectional composite structures. Chio and Yuan [9] investigated the time-dependent deformation of a pultruded glass fiber reinforced polymer (GFRP) composite. They concluded that Findley's power law model [10] can be successfully used to estimate the time-dependent deformation

* Corresponding author.
E-mail address: Ghasemi@kashanu.ac.ir
DOI: 10.22075/MACS.2018.12562.1125

of pultruded GFRP composite columns. Papanicolaou et al. [11] described the effect of fiber orientation on the nonlinear viscoelastic response of a unidirectional fiber polymeric composite. Using Schapery's nonlinear single integral constitutive equation, the researchers characterized the off-axis viscoelastic behavior of carbon fiber reinforced polymer (CFRP) composite materials. The generic function described each of the nonlinear parameters. Muliana et al. [12] tested and verified the viscoelastic responses of off-axis glass/vinylester multilayered composites under combined thermomechanical loadings. They performed isothermal creep tests under various stresses and temperatures on axial, transverse, and 45° off-axis specimens. They used the thermomechanical viscoelastic behaviors in order to characterize the time-stress-temperature dependent properties of the material and to predict the long-term behaviors of the composite [12]. Sawant and Muliana [13] introduced a numerical algorithm for the nonlinear thermomechanical viscoelastic analysis of orthotropic composite materials. Using Schapery's nonlinear single integral form, the effects of stress and temperature were considered along with the elastic and time-dependent material properties, which allowed for the prediction of time-dependent responses under general stress and temperature histories. Muddasani et al. [14] performed experimental work and a finite element analysis of nonlinear thermo-viscoelastic behaviors of multilayered composites. A nonlinear viscoelastic constitutive model based on the convolution integral equation for orthotropic materials was adopted. The nonlinear parameters in the equation were calibrated in the uniaxial isothermal creep tests for off-axis specimens and modeled as a function of the effective stress and temperature [14].

The laminated cylinder is one of a very few structural cases for which an exact elasticity solution is available. Guedes [15] analyzed the effect of the non-viscoelastic behavior of the polymer matrix on the mechanical behavior of thick multilayered cylinders. The proposed solution matched the exact solution for the pressurization of a compressive linear viscoelastic cylinder constrained by an elastic case. In addition, the viscoelastic effect on the time-dependent internal stress field was demonstrated. Faria and Guedes [16] discussed the possibility of reducing the test duration of a glass-fiber reinforced plastic (GFRP) piping system, while maintaining a final conclusion of long-term properties. Yoon and Oh [17] predicted the long-term performance of GRP pipes after 50 years based on failure pressure and time to failure using sustained internal pressure tests. Lavergne et al. [18] estimated the viscoelastic behavior and creep failure of E-glass fiber reinforced polyvinyl chloride (PVC). They used homogenization methods to obtained viscoelastic properties of PVC that reinforced of chopped glass fibers and random orientations. Poirette et al. [19] presented a new model that was based on the idea of a time-dependent damage spectrum; the researchers performed quasi-static, creep, and fatigue tests to characterize the elastic, viscoelastic, and plastic behaviors of the composite material. Yian et al. [20] investigated the effect of seawater absorption on the long-term viscoelastic response of glass/Bismaleimide composites. Monfared [21] used an analytical method to predict the creep behavior of fibrous composites under a tensile axial stress; the model showed good agreements between the results from the analytical and finite element methods.

The strain distribution in the wall of a composite cylinder, especially in the long-term, and the effect of lay-ups are very important. In this paper, a composite cylinder made of glass/vinylester with unidirectional fibers is subjected to internal pressure and studied using nonlinear viscoelastic approaches. Different theories and relations are used to investigate the long-term circumferential and radial strains in the cylinder wall, as well as the effect of the angle of the fibers on the distribution of the strains.

2. Creep Solution for the Composite Cylinder

A laminated cylinder made of glass/vinylester is shown in Fig. 1. The lay-ups are considered unidirectional for different orientations. The internal and external surfaces of the cylinder are insulated so that there is no loss of heat. In addition, the displacement conditions in the internal and external boundaries are free–free and the cylinder is closed at both ends.

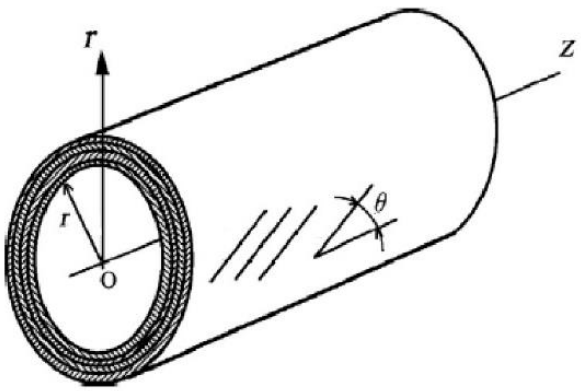

Figure 1. A composite cylinder with unidirectional fibers

After solving the homogeneous and particular solutions of the differential equation, the radial displacement relation for every layer can be written as follows:

$$\frac{d\sigma_{rr}}{dr}+\frac{\sigma_{rr}-\sigma_{\theta\theta}}{r}=0 \tag{1}$$

where σ_r and σ_θ are the axial and circumferential stresses, respectively. Considering the displacement-strain relations with the axial symmetry assumptions and the linear strain relation, the following equations are obtained:

$$\begin{aligned}\varepsilon_{rr}&=\frac{du}{dr}\\ \varepsilon_{\theta\theta}&=\frac{u}{r}\\ \varepsilon_{zz}&=o\end{aligned} \tag{2}$$

where ε_r, ε_θ and $\varepsilon_z$are the radial, circumferential, and axial strains, respectively, and u is the displacement in the radial direction. The Cartesian coordinates for the stress–strain relations in a unidirectional composite are:

$$\begin{bmatrix}\sigma_{11}\\ \sigma_{22}\\ \sigma_{33}\end{bmatrix}=\begin{bmatrix}C_{11}&C_{12}&C_{13}\\ C_{21}&C_{22}&C_{23}\\ C_{31}&C_{32}&C_{33}\end{bmatrix}\left\{\begin{bmatrix}\varepsilon_{11}\\ \varepsilon_{22}\\ 0\end{bmatrix}-\begin{bmatrix}\varepsilon_{11}\\ \varepsilon_{22}\\ 0\end{bmatrix}^{c}\right\} \tag{3}$$

where 1, 2 and 3 denote the different parameters in the x, y and z directions, respectively, and the superscript c specifies the creep strain. In addition, C is the modulus matrix with a nonlinear viscoelastic emphasis.

To convert the matrix from Cartesian coordinates to cylindrical coordinates, a transfer matrix is used, which is defined as follows [22]:

$$[A_{ij}]=\begin{bmatrix}m^4&n^4&0&2m^2n^2&0&0&4m^2n^2\\ m^2n^2&m^2n^2&0&m^4+n^4&0&0&-4m^2n^2\\ 0&0&0&0&m^2&n^2&0\\ n^4&m^4&0&2m^2n^2&0&0&4m^2m^2\\ 0&0&0&0&n^2&m^2&0\\ 0&0&1&0&0&0&0\end{bmatrix} \tag{4}$$

where $n=\cos\theta$, $m=sin\,\theta$ and θ is the fiber angle. Furthermore, the stress–strain relations in cylindrical coordinates can be obtained as:

$$\begin{bmatrix}\sigma_{rr}\\ \sigma_{\theta\theta}\\ \sigma_{zz}\end{bmatrix}=\begin{bmatrix}\bar{C}_{11}&\bar{C}_{12}&\bar{C}_{13}\\ \bar{C}_{21}&\bar{C}_{22}&\bar{C}_{23}\\ \bar{C}_{31}&\bar{C}_{32}&\bar{C}_{33}\end{bmatrix}\left\{\begin{bmatrix}\varepsilon_{rr}\\ \varepsilon_{\theta\theta}\\ 0\end{bmatrix}-\begin{bmatrix}\varepsilon_{rr}\\ \varepsilon_{\theta\theta}\\ 0\end{bmatrix}^{c}\right\} \tag{5}$$

By substituting Equation (2) into Equation (5), the stress-displacement relations for every layer can be obtained as:

$$\begin{aligned}\sigma_{rr}&=\bar{C}_{11}^{k}\frac{du}{dr}+\bar{C}_{12}^{k}\frac{u}{r}-\bar{C}_{11}^{k}\varepsilon_{rr}^{c}-\bar{C}_{12}^{k}\varepsilon_{\theta\theta}^{c}\\ \sigma_{\theta\theta}&=\bar{C}_{12}^{k}\frac{du}{dr}+\bar{C}_{22}^{k}\frac{u}{r}-\bar{C}_{12}^{k}\varepsilon_{rr}^{c}-\bar{C}_{22}^{k}\varepsilon_{\theta\theta}^{c}\\ \sigma_{zz}&=\bar{C}_{13}^{k}\frac{du}{dr}+\bar{C}_{32}^{k}\frac{u}{r}-\bar{C}_{13}^{k}\varepsilon_{rr}^{c}-\bar{C}_{32}^{k}\varepsilon_{\theta\theta}^{c}\end{aligned} \tag{6}$$

where the superscript k specifies the number of layers. By substituting Equation (6) into Equation (1), the equilibrium equation for each layer can be considered as follows:

$$\begin{aligned}&\frac{d^2(u_r)^k}{d^2r}+\frac{1}{r}\frac{d(u_r)^k}{rdr}-\frac{1}{r^2}\frac{\bar{C}_{22}^{k}}{\bar{C}_{11}^{k}}u_r=\\ &\frac{d\varepsilon_{rr}^{c}}{dr}+\frac{\bar{C}_{12}^{k}}{\bar{C}_{11}^{k}}\frac{d\varepsilon_{\theta\theta}^{c}}{dr}+\frac{1}{r}\frac{\bar{C}_{11}^{k}-\bar{C}_{12}^{k}}{\bar{C}_{11}^{k}}\varepsilon_{rr}^{c}\\ &+\frac{1}{r}\frac{\bar{C}_{12}^{k}-\bar{C}_{22}^{k}}{\bar{C}_{11}^{k}}\varepsilon_{\theta\theta}^{c}\end{aligned} \tag{7}$$

This equation has homogeneous and particular solutions.

$$u^k=u_h^k+u_p^k \tag{8}$$

Using linear elastic relations and axial symmetry assumptions, the equilibrium equation can be described as:

$$\begin{aligned}u=X_1^k r^B+X_2^k r^{-B}&+\frac{\frac{d\varepsilon_{rr}^{c}}{dr}+\frac{\bar{C}_{12}^{k}}{\bar{C}_{11}^{k}}\frac{d\varepsilon_{\theta\theta}^{c}}{dr}}{(16-(B^k)^2)}r^4\\ &+\frac{\frac{\bar{C}_{11}^{k}-\bar{C}_{12}^{k}}{\bar{C}_{11}^{k}}\varepsilon_{rr}^{c}+\frac{\bar{C}_{12}^{k}-\bar{C}_{22}^{k}}{\bar{Q}_{11}^{k}}\varepsilon_{\theta\theta}^{c}}{(9-(B^k)^2)}r^3\end{aligned} \tag{9}$$

To solve Equation (9), the creep strain values and the constant coefficients X_1^k and $X_2^k$are needed. To calculate the constant coefficients, the boundary conditions can be considered as follows:

$$\begin{aligned}u^k(r^k)&=u^{k+1}(r^k)\\ \sigma^k(r^k)&=\sigma^{k+1}(r^k)\end{aligned} \tag{10}$$

for $r=r_i\rightarrow {\sigma^1}_{rr}=-P_i$ and $r=r_o\rightarrow {\sigma^n}_{rr}=0$.

To obtain the creep strain parameters, the relation between the strains and the current stresses and the uniaxial creep behavior is based on the Prandtl–Reuss equations:

$$\begin{cases} \Delta\varepsilon_{rr}^{c} = \dfrac{\varepsilon_c}{2\sigma_e}(2\sigma_{rr} - \sigma_{\theta\theta} - \sigma_{zz}) \\ \Delta\varepsilon_{\theta\theta}^{c} = \dfrac{\varepsilon_c}{2\sigma_e}(2\sigma_{\theta\theta} - \sigma_{rr} - \sigma_{zz}) \end{cases} \quad (11)$$

where σ_e is the amount of octahedral stress:

$$\sigma_e = \frac{1}{3}\sqrt{(\sigma_{rr} - \sigma_{\theta\theta})^2 + (\sigma_{rr} - \sigma_{zz})^2 + (\sigma_{zz} - \sigma_{\theta\theta})^2} \quad (12)$$

In addition, ε_c is the creep strain obtained with the Schapery's single integral model at a constant temperature (25^oC) using the power method [23].

$$\varepsilon(t) = g_0 D_0 \sigma_e + g_1 g_2 D_1 (t/a_\sigma)^n \sigma_e \quad (13)$$

Using the expressed relations and Mendelson's approximation method [24] for a long period of time, the history of strains in time can be calculated. In this method, the thickness of the cylinder is divided into *K* divisions, as shown in Fig. 2.

It is assumed that the total time is sum of time increments throughout the progress of the creep process. For example:

$$t_i = \sum_{k=1}^{i-1} \Delta t_k + \Delta t_i \quad (14)$$

In addition, the values for $\Delta\varepsilon_{rr}^{c}$ and $\Delta\varepsilon_{\theta\theta}^{c}$ as the primary circumferential and radial strains, are considered for all K divisions. In the present study, initially $\varepsilon_{rr}^{c} = -0.00001$ and $\varepsilon_{\theta\theta}^{c} = 0.00001$. The strain for each time intervals is calculated by adding the previous strains with the new strain for all the thickness points of the cylinder. Ghasemi et al. [25] explained the numerical procedure.

3. Numerical Results and Discussion

Using the assumptions considered in the previous sections about creep solution and the nonlinear viscoelastic solution, the strain distribution in the cylinder wall for different time intervals is obtained. Table 1 shows the properties of a composite cylinder made of glass/vinylester with orthotropic properties using the Schapery coefficients for glass/vinylester.

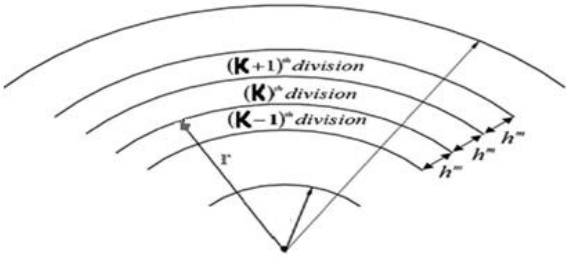

Figure 2. Division of the cylinder wall

Table 1. Elastic properties of the glass/vinylester composite cylinder [12]

Modulus (MPa)				Poisson's ratio	
E_{11}	E_{22}=E_{33}	G_{12}=G_{13}	G_{23}	ν_{12}=ν_{13}	ν_{23}
19268	13210	4572	3700	0.31	0.35

Furthermore, the composite cylinder is unidirectional at different orientations of $\theta = 45°$ and 90°; the cylinder is hollow with an interior radius r_i = 0.1 m, outer radius r_o = 0.12 m and interior pressure P_i = 5 MPa.

Because the nonlinear parameters depend on the stress, to calculate these parameters in the Schapery constitutive equation for the reference temperature (25°C), the following equation can be used for the glass/vinylester composite [12]:

$$\begin{aligned} g_0(\sigma_e) &= 1.004\mathrm{e}^{\sigma_e 5.655\times10^{-4}} \\ g_1(\sigma_e) &= 3.55\times10^{-3}\sigma_e + 0.878 \\ g_2(\sigma_e) &= 9.83\times10^{-6}{\sigma_e}^2 + 9.77\times10^{-3}\sigma_e + 0.636 \\ a_{\sigma_e} &= 1 \end{aligned} \quad (15)$$

The linear parameters in Equation (13) are shown in Table 2 for different angles [14].

3.1. Solution of the Time-Dependent Creep Strain Distribution

In this section, time-dependent creep behavior is studied for a unidirectional composite cylinder under internal pressure. To determine the composite behavior, the composite is considered to be nonlinear viscoelastic material in Schapery's single integral method, which is a function of temperature, time, stress, and fiber lay-up. However, all analyses are considered for ambient temperature. The time-dependent Mendelssohn numerical approximation method is used to estimate the long-term behavior. Figs. 3 and 4 show the radial and circumferential creep strain distribution in a composite cylinder wall under internal pressure for different fiber orientations. In Figs. 3 and 4, the diagrams are almost parallel to each other. Moreover, the values of the radial and circumferential strains strongly converge over time.

The variations in circumferential creep strain in the cylinder wall at a fiber orientation of $\theta = 90°$ from 5 to 30 years are shown in Fig. 3 (a). The values of the circumferential creep strain on the inner surfaces vary from 1.31% to 1.98%. As the time increase, slop of circumferential creep strain reduced. The values of the circumferential creep strain on the outer surface are less than on the inner surface. In Fig. 3 (b), the values of the radial creep strains vary on the inner surface from –0.97% to –1.33%. As depicted, the slope of the strain variations increases from 5 years to 30 years.

Table 2. Viscoelastic linear parameters of glass/vinylester composite

Off-axis angle (θ)	45°	90°
$D_0*10^{-5}(1/MPa)$	0.79	0.81
$D_1*10^{-5}(1/MPa)$	0.16	1.35
n	0.20	0.189

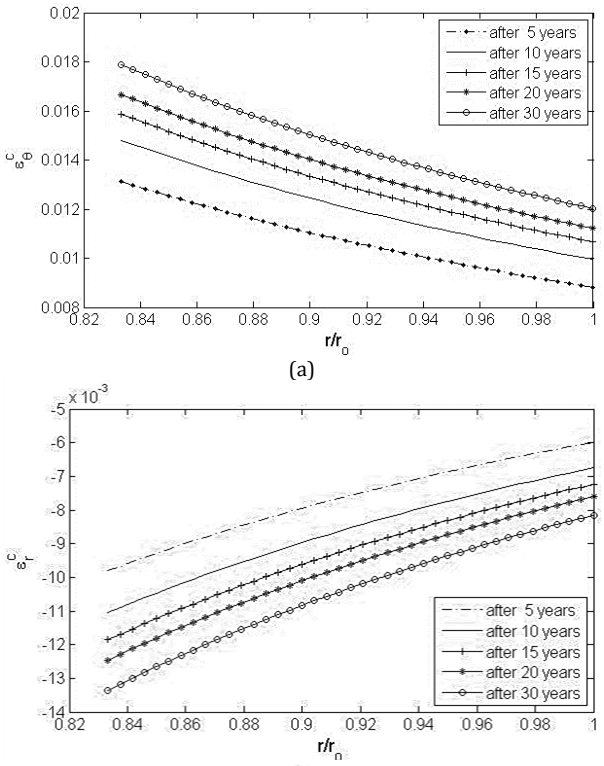

Figure 3. Diagram of circumferential creep strain (a) and radial creep strain (b) for the composite cylinder under internal pressure of the arrangement with the angel of $\theta = 90°$

And the absolute values of the radial creep strain increased with time. In addition, the values of the radial creep strain on the outer surface vary from –0.597% to –0.81%.

The variations of the circumferential creep strain in the cylinder wall at a fiber orientation of $\theta = 45°$ are shown in Fig.4 (a). The values of the strain range from 0.23% to 0.27% on the inner surface. The maximum and minimum strains on the inner surface occur at 30 and 5 years, respectively. Furthermore, the values of the strain gradually decrease over the years; the values of the strain on the outer surface vary from 0.15% to 0.21%.

The values of the radial strain, which are shown in Fig 4 (b), vary from –0.19% to –0.25% on the inner surface. According to the figure, the absolute values of the strain decrease from the inner surface toward the outer surface and vary from –0.22% to –0.29%.

To clarify the extent of the changes in creep strains, the values of the radial and circumferential creep strains on the inner, middle, and outer wall of the cylinder with fiber angles of $\theta = 90°$ and $\theta = 45°$ are shown in Table 3 and Table 4, respectively.

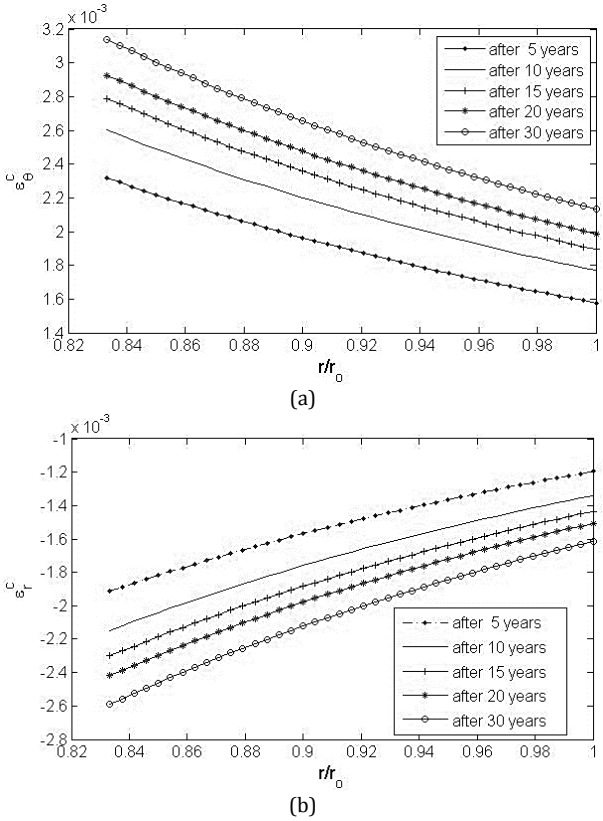

Figure 4. Diagram of circumferential creep strain (a) and radial creep strain (b) for the composite cylinder under internal pressure of the arrangement with the angel of $\theta = 45°$

Table 3. Values of radial and circumferential creep strain in the walls of a cylinder with a fiber orientation of $\theta = 90°$

Creep strain	Radius ratio	After the number of years				
		5	10	15	20	30
$\varepsilon_r^c(\%)$	0.833	-0.9798	-1.1050	-1.1860	-1.2410	-1.3360
	0.9083	-0.7753	-0.8743	-0.9378	-0.9856	-1.0750
	1.000	-0.5987	-0.6751	-0.7240	-0.7608	-0.8154
$\varepsilon_\theta^c(\%)$	0.833	1.3130	1.4800	1.5870	1.8770	1.9880
	0.9083	1.0820	1.2200	1.3080	1.374	1.4730
	1.000	0.8827	0.9952	1.0670	1.1210	1.2020

Table 4. Values of radial and circumferential creep strain in the walls of a cylinder with a fiber orientation of $\theta = 45°$

Creep strain	Radius ratio	After the number of years				
		5	10	15	20	30
$\varepsilon_r^c(\%)$	0.8333	-0.1913	-0.2148	-0.2301	-0.2417	-0.2592
	0.9083	-0.1532	-0.1791	-0.1840	-0.1913	-0.2072
	1.000	-0.1196	-0.1341	-0.1435	-0.1507	-0.1615
$\varepsilon_\theta^c(\%)$	0.833	0.2317	0.2600	0.2785	0.2926	0.3138
	0.9083	0.1924	0.2159	0.2311	0.2427	0.2602
	1.000	0.1578	0.1769	0.1893	0.1988	0.2131

3.2. Validation of study

The present study has not been founded on any research about the time-dependent creep strain in laminated composite or pressure vessels. You et al. [26] studied the steady-state creep in FGM cylindrical vessels under internal pressure and in homogeneous radially polarized anisotropic piezoelectric material. Fig. 5 shows the dimensionless radial stresses over 10 years in the wall of a cylinder with a fiber angle of $\theta = 45°$, which are based on the solution by You et al. [26] for the case of a zero material constant (i.e., homogeneous material). Considering the very similar radial stresses obtained in both approaches, the correctness of the present solution may be verified in this respect.

4. Conclusion

In this study, the distribution of long-term creep strain in a composite cylinder under internal pressure was investigated for different fiber orientations. Nonlinear viscoelastic approaches were used to study the distribution of the stresses and long-term creep strain. The distribution of long-term circumferential and radial strains in the cylinder wall and the effect of the fiber orientations on the distribution were considered using Schapery's single integral model, Prandtl–Reuss relation, and Mendelson's approximation method.

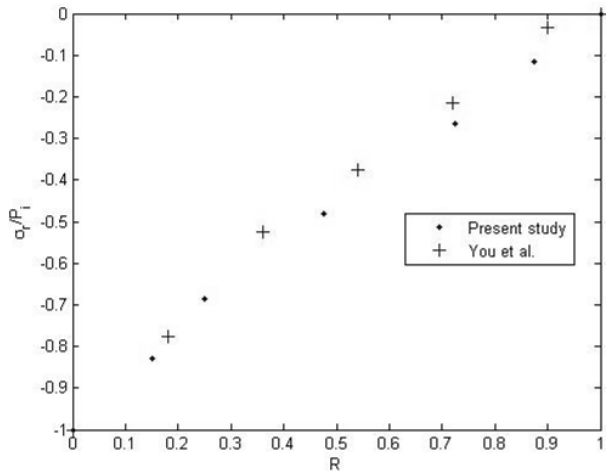

Figure 5. Dimensionless radial stress variations in the wall of a composite cylinder

The obtained results indicate that the parameters of fiber orientation, dimension radius, and time have considerable effects on the distribution of long-term creep strain in a composite cylinder

The results show that the values of creep strain for a fiber angle of $\theta = 45°$ are less than at a fiber angle of $\theta = 90°$. The values of creep strain at a specific fiber angle over time indicate that as time increases, the absolute values of the creep strain increase. The values of the creep strains decrease from the inner surface toward the outer surface.

References

[1] Arefi M. Thermo-elastic analysis of a rotating hollow cylinder made of arbitrary functionally graded materials*. J Theorical and Applied Mechanic* 2015; 45: 41–60.

[2] Loghman A, Nasr M and Arefi M. Nonsymmetric thermomechanical analysis of a functionally graded cylinder subjected to mechanical, thermal, and magnetic loads. J of Thermal Stresses 2017; 40(6): 765-782.

[3] Tsukrov I and Drach B. Elastic deformation of composite cylinders with cylindrical orthotropic layers. *Int J Solids and Structure* 2010; 47: 25-33.

[4] Zhang Q, Wang ZW, Tang CY, Hu DP, Liu PQ and Xia LZ. Analytical solution of the thermo-mechanical stresses in a multilayered composite pressure vessel considering the influence of the closed ends. *Int J Pressure Vessels and Piping* 2012; 98: 102-110.

[5] Ghasemi AR, Kazemian A and Moradi M. Analytical and numerical investigation of FGM pressure vessel reinforced by laminated composite materials. *J Solid Mechanic* 2014; 6(1): 43-53.

[6] Arefi M, Koohi Faegh R and Loghman A. The effect of axially variable thermal and mechanical loads on the 2D thermoelastic response of FG cylindrical shell. *J Thermal Stresses* 2016; 39(12): 1539-1559

[7] Arefi M, Abbasi AR and Vaziri Sereshk MR. Two dimensional thermoelastic analysis of FG cylindrical shell resting on the Pasternak foundation subjected to mechanical and thermal loads based on FSDT formulation. *J Thermal Stresses* 2016; 39: 554-570

[8] Violette MG and Schapery RA. Time-dependent compressive strength of unidirectional viscoelastic composite materials. *Mechanic Time-Dependent Material* 2002; 6: 133-145.

[9] Chio Y and Yuan RL. Time-dependent deformation of pultruded fiber reinforced polymer composite columns. *J Composite for Construct* 2003; 7(4): 356-362.

[10] Findley WN. Mechanism and mechanic of creep of plastic. *J Polymer Engineerin* 1960; 16: 57-65.

[11] Papanicolaou GC, Zaoutsos Sp and Kontou EA. Fiber orientation dependence of continuous carbon/epoxy composites nonlinear viscoelastic behavior. *Composite Science and Technology* 2004; 64: 2535-2545.

[12] Muliana A, Nair A, Khan KA and Wagner S. Characterization of thermo-mechanical and long term behaviors of multi-layered composite materials. *Composite Science and Technology* 2006; 66: 2907-2924.

[13] Sawant S and Muliana A. A thermo-mechanical viscoelastic analysis of orthotropic materials. *Composite Structres* 2008; 83: 61-72.

[14] Muddasani M, Sawant S and Muliana A. Thermo-viscoelastic responses of multilayered polymer composite experimental and numerical studies. *Composite Structures* 2010; 92: 2641-2652.

[15] Guedes RM. Nonlinear viscoelastic analysis of thick-Walled cylindrical composite pipes. *Int J Mechanic Science* 2010; 52: 1064-1073.

[16] Faria H and Guedes RM. Long-term behaviour of GFRP pipes: Reducing the prediction test duration. *Polymer Testing* 2010; 29: 337–345.

[17] Yoon SH and Oh JO. Prediction of long term performance for GRP pipes under sustained internal pressure. *Composite Structure* 2015; 134: 185–189

[18] Lavergne F, Sab K, Sanahuja J, Bornert M and Toulemonde C. Estimation of creep strain and creep failure of a glass reinforced plastic by semi-analytical methods and 3D numerical simulations. *Mechanic of Materials* 2015; 89: 130–150.

[19] Poirette Y, Dominique P and Frédéric T. A contribution to time-dependent damage modeling of composite structures. *Appiled Composite Materials* 2014; 21(4): 677-688.

[20] Yian Z, Zhiying W, Keey SL and Boay CG. Long-term viscoelastic response of E-glass/Bismaleimide composite in seawater environment. *Appied Composite Materials* 2015; 22(6): 693-709.

[21] Monfared V. Circular functions based comprehensive analysis of plastic creep deformations in the fiber reinforced composites. *Appied Composite Materials* 2016:1-13.

[22] Xia M, Takayanagi H and Kemmochi K. Analysis of multi-layered filament-wound composite pipes under internal pressure. *Composite Structure* 2001; 53: 483-491.

[23] Lou YC, Schapery RA, Viscoelastic characterization of a nonlinear fiber-reinforced plastic. *J Composite Materials* 1971; 5:208-234.

[24] Mendelson A. Plasticity: theory and applications. New York: Macmillan. 1968.

[25] Ghasemi AR, Hosseinpour K, Mohandes M. Modelling creep behavior of carbon-nanotubes/fiber/polymer composite cylinders. *Part N: J Nanomaterials, Nanoengineering and Nanosystems* 2017, DOI: 10.1177/2397791418768576

[26] You H, Ou H, Zheng ZY. Creep deformation and stresses in thick-walled cylindrical vessels of functionally graded materials subjected to internal pressure. *Composite Structures* 2007; 78: 285–91.